Patient-Specific Guides: Improved Point-Registration Accuracy for Surgical Navigation and Robotic-Assisted Surgery

Jedediah K. White

A thesis

submitted in partial fulfillment of the

requirements for the degree of

Master of Science in Bioengineering

University of Washington

2017

Committee:

Randal P. Ching, Chair

Ernest U. Conrad III

Matthew O'Donnell

Program Authorized to Offer Degree:

Bioengineering

University of Washington

Abstract

Patient-Specific Guides: Improved Point-Registration Accuracy for Surgical Navigation and Robotic-Assisted Surgery

Jedediah Keith White

Chair of the Supervisory Committee:
Randal P. Ching, Research Associate Professor
Mechanical Engineering

Image-based surgical navigation offers improved integration of preoperative planning with intraoperative execution and documentation. Registration is a fundamental step in all surgical navigation procedures and entails the alignment of preoperative image map with intraoperative physical anatomy. While implanted fiducial markers are the gold standard for registration, they either require an extra procedure or intraoperative imaging that add time and cost to the course of care. It is imperative to find an alternative that reduces the burden on patient, clinician, and the health care system. Paired-point matching using anatomic landmarks and surface mapping have been used as alternatives, but distinct landmarks or surfaces are needed for their effectiveness. A patient-specific point-registration guide was thus developed and evaluated for accuracy and precision in an idealized model. Results were encouraging and further work is recommended.

TABLE OF CONTENTS

LIST OF FIGURES

LIST OF TABLES

ACKNOWLEDGEMENTS

I sincerely thank my advisor, Dr. Randy Ching, for his continued support through this process. Randy, I very much appreciate your mentorship, both personal and professional, and have been fortunate to have you as a friend and advisor. I would also like to thank Dr. Chappie Conrad, as he's supported not only this project, but my development as a person and scientist over the last ten years. Chappie, I'm very grateful for you and all that you've done for me. I also thank Dr. Matt O'Donnell. Dr. O'Donnell, your course on technology commercialization inspired and motivated me. Thank you for agreeing to be on my committee and for your generous input. I also sincerely thank Stephanie Punt. Stephanie, your help with the statistical analysis and manuscript edits has been invaluable, but more importantly, you've been a great friend to me throughout this process. Thank you. Finally, I would like to thank Blake Gibbons from Stryker Navigation. Blake, thank you for your unwavering support for this project and for always making sure I had whatever I needed to successfully complete my mission.

Chapter 1. INTRODUCTION

Biomedical innovation is very much a story of technology and technique, a narrative of their development and the interplay that exists between them. Wilhelm Conrad Röntgen first described x-rays in a paper submitted on December 28, 1895; within two months a Birmingham, England casualty surgeon, J. Hazelwood Clayton, had already used a radiograph to guide the removal of a sewing needle from a woman's hand (Burrows, 1986; Rowland, 1896). The first image-guided surgery on record, it also clearly illustrates the intimate connection between technological advancement and growth of technique.

Humans create and leverage tools to accomplish a desired result with greater power and efficiency. Biomedical innovation, a form of tool building, allows for expansion and enhancement of a clinician's diagnostic and therapeutic capability. The discovery and utilization of x-rays is just one example of this rapidly accelerating process. Subsequent developments in imaging, as well as with devices such as the endoscope (e.g., the bronchoscope) and electrograph (e.g., the electrocardiograph), further demonstrate the role of tools in extending or augmenting the clinician's natural faculties.

Although the introduction of innovative technologies and techniques has transformed diagnostic and therapeutic capability, integration of the various multidisciplinary care components remains relatively unsophisticated. This lack of sophistication is revealed in the relationship between imaging and surgery. Devices like computed tomography (CT), magnetic resonance imaging (MRI), and positron emission tomography (PET) are powerful tools for improved visualization and planning, and have consequently become an invaluable component of the surgeon's toolset. However, translation to the operating room (OR) continues to be a

significant challenge and most surgical procedures make relatively rudimentary use of the available imaging modalities. A typical surgical plan will be informed by the surgeon's qualitative assessment of the relevant imaging, but while this may provide a general sense of the anatomical and molecular extent of disease, the surgeon must still fundamentally rely on his/her visual and tactile surgical skill in the OR.

1.1 IMAGE-BASED SURGICAL NAVIGATION

Image-based surgical navigation, also referred to as image-guided surgery (IGS), is a promising technology for augmenting interventional capability. Functioning in a similar manner to GPS (global positioning system), this tool enables the surgeon to use a preloaded "map" of the patient, in this case the patient's preoperative imaging (CT, MRI, PET, etc.), to guide the surgical procedure. Navigation offers improved integration of preoperative planning with intraoperative execution and documentation, and is especially advantageous in cases where important anatomical features (e.g., tumors) may not be readily visible or when implant malalignment is of concern.

1.1.1 *Historical Development*

Modern surgical navigation systems and techniques have their origin in the stereotactic frame, a tool that embodies a foundational image-guided surgery concept: alignment of image space (i.e., the preoperative "map") with physical space (i.e., the intraoperative patient anatomy) (Galloway, 2001). Horsley and Clarke are credited with the innovation and in 1908 they gave a detailed account of the device and its use in studying the monkey cerebellum (Horsley & Clarke, 1908), but it took almost 40 years before Spiegel et al. sufficiently improved upon the design and opened the way for clinical applications (Spiegel, Wycis, Marks, & Lee, 1947). It was not until

the advent of CT scanning and the personal computer, however, that transformative change came to the field of surgical navigation (Cleary & Peters, 2010). Whereas classic stereotaxy used images to find physical locations, rapidly growing computational power and the 3D data provided by CT allowed for visualization in image space via tracking in physical space (i.e., frameless stereotaxy) (Galloway, 2001). These innovations gave rise to the first truly modern surgical navigation systems and by the late 1980s and early 1990s devices for 3D localization (i.e., tracking) on a single image plane (Friets, Strohbehn, Hatch, & Roberts, 1989; Kosugi et al., 1988; Roberts, Strohbehn, Hatch, Murray, & Kettenberger, 1986; Watanabe, Watanabe, Manaka, Mayanagi, & Takakura, 1987) and three orthogonal planes (Galloway, Edwards, Lewis, & Maciunas, 1993; Maciunas et al., 1992) had been developed.

1.1.2 *Applications*

Surgical navigation has primarily been used in neurosurgery, oral and maxillofacial surgery, orthopaedic surgery, and otolaryngology-head and neck (ENT) surgery where the relative stasis of the surrounding bony structures ensures consistent registration between imaging and anatomy throughout the entire procedure. However, navigation has potential applicability to a broad range of fields including breast, cardiothoracic, hepatic (liver), prostate, renal (kidney), and various other soft tissue interventions. Surgical navigation currently serves three distinct purposes: confirmation of intraoperative anatomic location or a "wayfinding" function, confirmation of the position or orientation of a medical device or reconstructive component, and surgical margin assessment and boundary definition (i.e., amount of normal tissue surrounding a tumor) in surgical oncology procedures.

In orthopaedics, the technology has been utilized extensively for trauma, arthroplasty, and spine surgery. Its use in those disciplines illustrates its potential as a wayfinding function, which

is attractive in more complicated anatomic locations (i.e., spine and pelvis), and for confirming the reconstructive component's orientation; for example, confirming the inclination, center of rotation, and version of an acetabular component in total hip arthroplasty, the adequacy of reduction in pelvic fractures, or the precise placement of pedicle screws in spinal surgery. In orthopaedic oncology, surgical navigation serves the additional purpose of providing documentation of the surgical resection and reconstruction (e.g., tumor margins in osteosarcoma resections).

1.1.3 *Components*

Image-based surgical navigation systems and techniques share four common components: 1) preoperative imaging (provides the GPS "map" for the navigation system), 2) localization or tracking (delivers real-time monitoring and feedback of the patient's anatomy and the position/orientation of tools and instruments in the surgical field, 3) registration (aligns the image-map with the patient's anatomy in the operating room), and 4) visualization (displays position/orientation of tools and instruments relative to the image-map). Steps 1, 2, and 4 have been well established using highly standardized medical imaging systems, formats (i.e., DICOM), and 3D reconstruction techniques (e.g., volume rendering) in conjunction with advanced optical or electromagnetic spatial tracking systems. Registration, however, has proven to be the "weakest link" and most troubling step in implementing surgical navigation (Fitzpatrick, 2010).

1.1.4 *Registration*

Registration entails the intraoperative alignment of the patient's preoperative imaging scans (typically either CT or MRI) to his/her physical anatomy in the OR to provide a one-to-one

correspondence (or mapping) of the image space to the physical space (**Figure 1.1**). Successful completion of this step allows the surgeon to accurately navigate the patient's anatomy, using image-guidance to implement the surgical plan. Registration (in)accuracy is perhaps the single most important issue preventing wider adoption and confidence in surgical navigation, as poor registration can lead to costly delays and potentially dangerous outcomes.

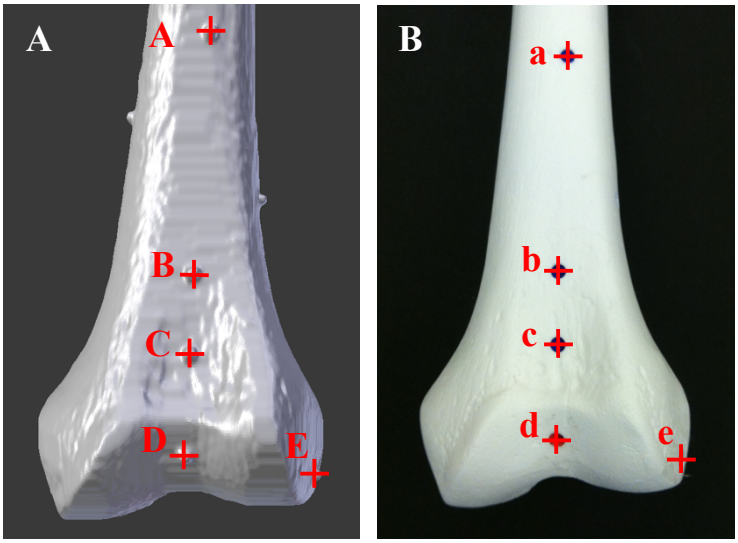

Figure 1.1. Registration in surgical navigation: the alignment of image space with physical space.

(A) Pre-planned registration points (A-E) on the surface of a CT-based image model of a Sawbones femur. (B) During surgery, the physical locations of the pre-planned points (A-E) must be identified by the surgeon on the physical anatomy such that the physical points (a-e) exactly match the locations of virtual (pre-planned) to obtain a successful registration. If done correctly, this will result in good alignment of the physical anatomy with the image-based (virtual) anatomy, thus enabling the surgeon to navigate using the image-based model during surgery.

Numerous registration techniques have been explored to improve registration accuracy (**Table 1.1**). Feature-based methods encompass point-based, contour-based, and surface-based approaches and are most common. Paired-point registration using fiducial markers is the most accurate method and considered to be the "gold standard," but it is also the most invasive and

requires an additional initial procedure to preoperatively implant the fiducial markers prior to imaging. The more common practice is to use landmark registration where the surgeon chooses anatomical landmarks (e.g., a bony prominence) that can be identified on both the imaging and the physical anatomy. Unfortunately, this technique has been shown to be highly inaccurate (Yau et al., 2007). Unlike point-based methods, surface registration relies on matching an anatomical region found in both the OR and reconstructed image-map. While using surfaces removes the need for identifying difficult to find anatomical landmarks, the technique requires sufficient feature depth and still does not approach the accuracy of fiducial marker registration. Alternatively, a registration scan can be obtained intraoperatively using an OR scanner; however, this usually requires significant additional radiation exposure and/or costly OR time. A technology that achieves the accuracy of fiducial paired-point registration without the invasiveness or high-added costs offers great potential in furthering surgical navigation technology.

Table 1.1. Registration techniques for image-based surgical navigation. (Hajnal, Hawkes, & Hill, 2001; Liao, Zhang, Sun, Miao, & Chefd'hotel, 2013; Markelj, Tomaževič, Likar, & Pernuš, 2012)

Method	**Classification**	**Intraoperative data source**
3D/3D image-to-physical registration		
Paired-point matching	Point-based	Anatomical landmarks or fiducial markers
Surface matching	Surface-based	Point cloud on anatomical surface
3D/2D image-to-image registration		
Projection-to-Volume	Point-based Contour-based Gradient-based Intensity-based	X-ray fluoroscopy images
Slice-to-Volume	Surface-based	2D ultrasound images
Video-to-Volume	Surface-based	Endoscopic video output
3D/3D image-to-image registration		
Surface matching	Surface-based	3D scanner surface data
Volume-to-Volume	Feature-based Intensity-based	CBCT, CT, MRI, or 3D ultrasound images

1.2 Preliminary Studies

The Orthopedic Oncology Service at Seattle Children's Hospital (SCH) first began using surgical navigation in 2010. Most of the cases involved children with sarcoma, a cancer of the connective tissues that often requires radiation therapy as an adjuvant to surgery. Therefore, the decision was made to limit additional radiation exposure (by not employing an intraoperative scanner) and anatomical landmarks were selected as the registration method of choice. Unfortunately, this approach proved inconsistent and frequently resulted in poor image and physical space alignment. As a result, the present work was undertaken to develop an improved registration technique.

This effort was launched in conjunction with two preliminary research studies at SCH and the University of Washington (UW) Applied Biomechanics Laboratory (ABL). The first study, conducted at SCH, examined the error associated with anatomical landmark registration during actual tumor resection surgeries. Subsequent work in the UW ABL focused on establishing the baseline accuracy and precision of the Stryker Navigation System II (Stryker; Kalamazoo, MI, USA), the same bidirectional infrared surgical navigation system that was used at SCH, prior to further experimentation. Both studies are briefly summarized below.

1.2.1 *Study 1: Assessment of Registration Accuracy During Image-Guided Oncologic Limb-Salvage Surgery*

The main purpose of this study was the evaluation of registration accuracy in a clinical setting, as well as the validation of the "system reported error" (SRE) reported by the navigation system (Stoll et al., 2015). From November 2012 to July 2013, eight image-based surgical navigation procedures performed by the Orthopedic Oncology Service at SCH were reviewed. Anatomical paired-point registration (with surface matching) was utilized for each case. Anatomic landmarks used for registration were resampled and digitized following alignment of the physical space with image space for subsequent comparison with the corresponding planned registration point coordinates from the virtual anatomy.

Registration accuracy was defined as the mean measurement error (ME) between planned and post-registration point coordinates. The difference was 12.21 ± 6.52 mm, a significantly higher value than the mean SRE of the Stryker Navigation System (0.68 ± 0.15 mm; $p = .002$). Registration via anatomic landmarks was shown to result in a substantial shift between planned and post-registration point coordinates, a shift that is not captured by SRE. Anatomical landmark registration was thus deemed too inaccurate for reliable use in a clinical setting.

1.2.2 *Study 2: Establishment of Baseline Accuracy and Precision for a Commercial Surgical Navigation System*

This study assessed the influence of several alterable factors on the baseline accuracy and precision of the Stryker Navigation System in an idealized setting (Gundle, White, Conrad, & Ching, 2017). Specifically, the effect of camera position, patient tracker position, and number of active markers on the patient tracker were evaluated by changing the distance between the camera and target region (150 cm, 200 cm, and 247 cm), the distance between the patient tracker and target region (20 cm, 30 cm, and 40 cm), and the number of actively functioning bidirectional markers (all markers active vs. the minimum). Parameters were varied to simulate surgical working conditions. The study employed a calibrated grid as the target with known distances between precision-machined indentations, which were used to gather a sequence of points for each of the 18 trials (**Figure 1.2**).

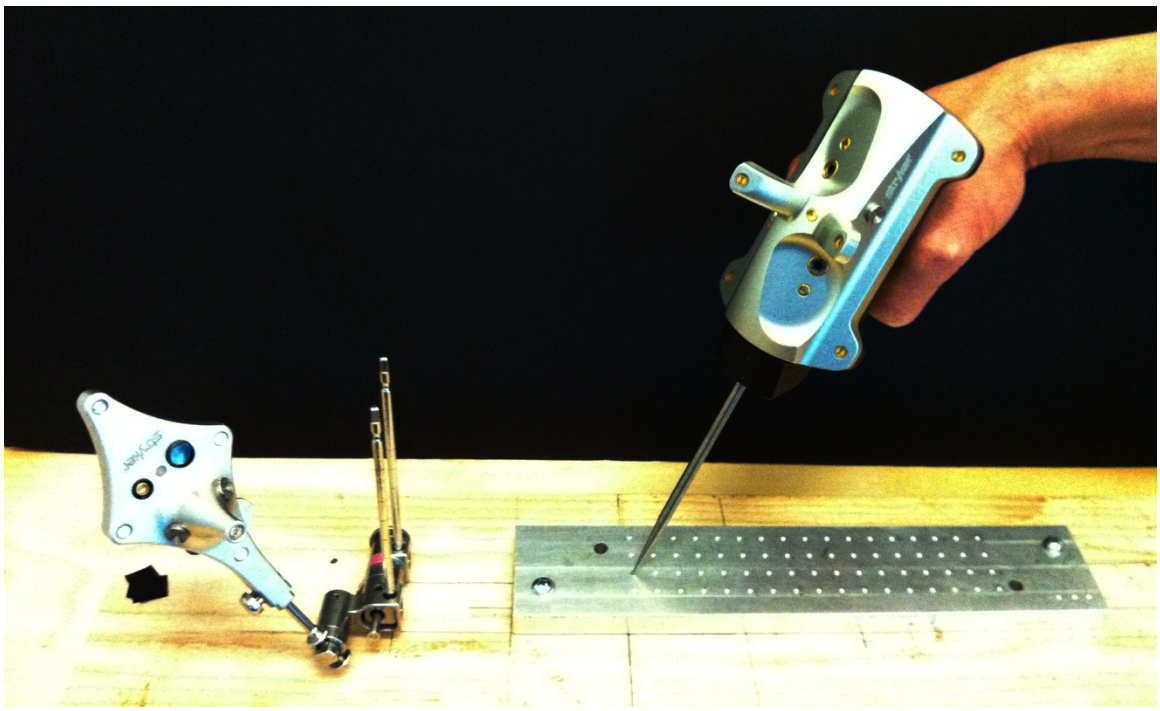

Figure 1.2. Calibrated grid (target) for baseline accuracy and precision assessment. A precision CNC-milled grid was used to examine the accuracy and precision of the Stryker Navigation System when varying the distance to the camera, distance to the patient tracker, and the number of active infrared markers.

Accuracy was assessed using a series of measurements, calculated from the collection of digitized point coordinates. Measured distances ranged from 10 to 120 mm with twelve measurements taken for each distance. Values determined by the navigation system were compared to the actual distances, as defined by a MicroScribe M digitizing system (Solution Technologies, Inc.; Oella, MD, USA), and the root mean square (RMS) error used as the primary outcome variable for accuracy. Precision was evaluated using four indentations at the outer corners of the target space. Each indentation was digitized an additional five times while varying the orientation of the navigation system pointer, with the primary outcome variable for precision defined as the standard deviation of the mean for multiple (5) repeated measurements.

Subsequent analysis revealed a significant decrease in accuracy ($p < .001$) and precision ($p = .005$) when the distance between camera and target was increased. Limiting the number of active infrared markers also significantly decreased accuracy ($p = .03$) and precision ($p < .001$), while the location of the patient tracker did not have a serious impact. In addition to establishing a baseline for system accuracy and precision, these findings underscore the importance of the OR setup (i.e., minimizing the distance between the camera and trackers, and maximizing the number of markers seen by the cameras) and suggest the need for software changes to improve clinical performance.

1.3 Patient-Specific Point-Registration Guide for Improved Accuracy

Computer-aided surgery (CAS), often used interchangeably with surgical navigation and IGS, also encompasses the use of imaging for applications such as the creation of patient-specific implants and guides. This implementation utilizes the preoperative image in conjunction with computer-aided design (CAD) software and rapid prototyping technologies to segment and model the relevant anatomy, before design and manufacture of the desired prosthetic or tool. Our team has developed a patient-specific surgical navigation registration technique for bony anatomy that will enable consistently accurate registration at low monetary and radiation cost (Ching, White, & Conrad, 2016).

1.3.1 *Background*

While patient-specific templates show potential in a variety of fields, most of the work has been directed towards oral, maxillofacial, and orthopaedic applications. Precursors to our technique can be found in the patient-specific surgical guide and dental splint registration device. Both are

briefly outlined below, along with other attempts at developing a patient-specific registration tool.

The goal of the patient-specific surgical guide is to incorporate preoperative imaging and operative plan into a personalized template that can be used without the need for intraoperative imaging or surgical navigation. In orthopaedics, this device would typically be employed for drill (e.g., pedicle screw placement) or resection (e.g., total knee arthroplasty) guidance. While showing promise, these tools do not provide the flexibility of surgical navigation and are best utilized in specific circumstances or in concert with intraoperative imaging.

Registration via dental splint does not necessarily require CAD modeling and rapid prototyping. Nevertheless, it too relies upon the production of a patient-specific template, in this case a dental splint with implanted fiducials or attached registration frame (G Eggers, Mühling, & Marmulla, 2006). The device is attached prior to preoperative imaging and again intraoperatively for the registration component of the surgical navigation procedure. After registration, the splint is either removed or utilized for patient tracking.

Matsumoto et al. eventually integrated the patient-specific surgical guide and dental splint registration device concepts, developing what they would call the surface template-assisted marker positioning (STAMP) method for otologic surgery (Matsumoto, Hong, Hashizume, & Komune, 2009). Their technique worked like a patient-specific drill guide, but instead of guiding screw placement, it directed a navigation probe towards the chosen registration points. The group would go on to refine their approach with promising results in simulation studies (Oka et al., 2014; Yamashita et al., 2016). Jang and Lee described a similar method for total knee arthroplasty and reported positive findings when analyzing the attachment errors associated with

such a device (Jang & Lee, 2014). Other than these few examples, there does not appear to be any additional literature on the topic.

1.3.2 *Development of the Patient-Specific Point-Registration Guide*

Our method creates a patient-specific point-registration guide based on preoperative imaging. Using image segmentation software, a 3D computer model is created of the patient's relevant bony anatomy in a region that will be exposed during the planned surgery. From this anatomical computer model, a CAD model is made of a patient-specific guide that will enable pre-picked registration points on the patient's bony anatomy to be easily and repeatably digitized during surgery. The CAD model of the point-registration guide is then rapid prototyped (3D printed), sterilized, and delivered to the OR for the surgery. The use of this guide will provide more accurate and rapid point-based registration thereby improving the reliability and adoption of surgical navigation. **Table 1.2** provides a comparison of the potential benefits of using a patient-specific registration guide over other current technologies and techniques.

Table 1.2. Patient-specific registration guide: comparison between proposed attributes.

Attribute	**Patient-specific guide**	**Fiducial marker ("gold std.")**	**Intraoperative imaging**	**Anatomical landmark**
Accuracy	+	+	+	–
Cost	+	–	–	+
Risk				
- Added procedure	+	–	+	+
- Added radiation	+	+	–	+
Time	+	–	+	–

Chapter 2. METHODS

A verification study was performed on an anatomic Sawbones (Pacific Research Laboratories; Vashon Island, WA, USA) model to demonstrate both the accuracy and precision of the navigation guide technology. Registration and target accuracy were assessed for anatomic landmark registration (standard practice), fiducial marker registration ("gold standard"), and the patient-specific guide for registration. Points were repeatedly digitized and used to establish the precision of each technique. This provided baseline data in an idealized model (with no soft-tissue artifact), as well as the opportunity to develop the procedure for producing registration guides on plastic models (with no biosafety concerns) before moving to biological tissues. The verification study was performed using a distal femur model, an anatomical location where bone tumor resections are commonly performed.

The following is hypothesized: 1) the 3D-printed point-registration guide will significantly improve registration and target accuracy compared to anatomic landmark registration (both with and without surface matching), and have comparable accuracy to fiducial marker registration; and 2) localization of 3D-printed guide points will approach the precision of fiducial marker localization and both techniques will be more precise than localization of anatomic landmarks.

2.1 Preparation and Setup

2.1.1 *Sawbones Femur Preparation*

A Sawbones femur model was prepped for 4 mm fiducial bead placement. Using a burr, nine 4 mm diameter hemispheres were carved from the distal portion of the femur: three to be used for fiducial registration and six to assess target accuracy for each of the registration techniques (**Figure 2.1**). Fiducial registration markers were positioned near the most commonly used

anatomical landmark registration locations; i.e., the medial epicondyle, lateral epicondyle, and deepest point of the trochlear groove. A typical distal femoral tumor occurs in the metaphysis and/or diaphysis, and the fiducial targets were placed in a manner that reflected this common clinical presentation. The six target markers were placed 2-12 cm proximal to the epicondyles at 2 cm intervals. Four of the fiducial targets were on the anterior surface of the Sawbones, with the other two positioned on the lateral and medial side of the model, respectively, to simulate depth of use in the clinical context. Tape was used to affix the 4 mm fiducial beads to the carved surfaces and the femur model underwent a high resolution axial CT study (i.e., 0.625 mm slice thickness).

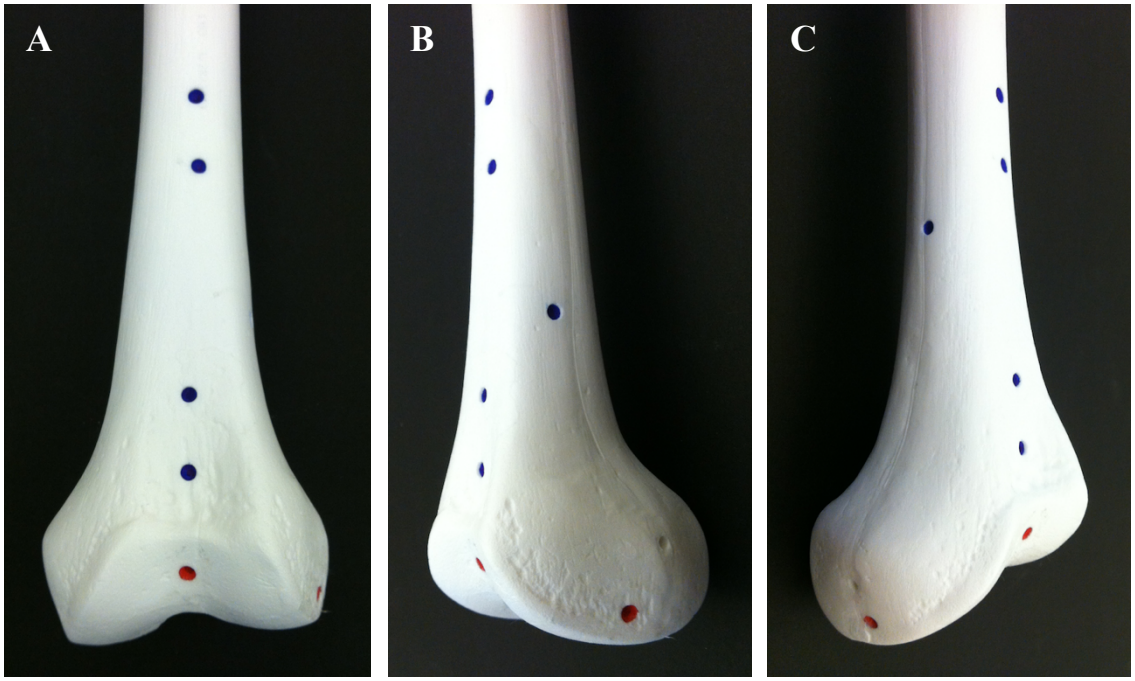

Figure 2.1. Sawbones femur model with distal portion prepped for fiducial bead placement and CT scan.

(A) Anterior, (B) lateral, and (C) medial views. Red dots signify locations used for fiducial marker registration while blue dots are those used for assessment of target accuracy.

2.1.2 *Point-Registration Guide Preparation*

After the Sawbones model was imaged, the DICOM files from the CT scan were loaded into a custom software package (SegVue, IS4D; Seattle, WA, USA) for segmentation. The resultant 3D mesh was exported in the STL file format and subsequently imported into a second open-source software, Blender (Blender Foundation; Amsterdam, Netherlands), for creation of a virtual image of the point-registration guide. **Figure 2.2** shows an image slice from the CT study with a surface rendering of the associated 3D mesh.

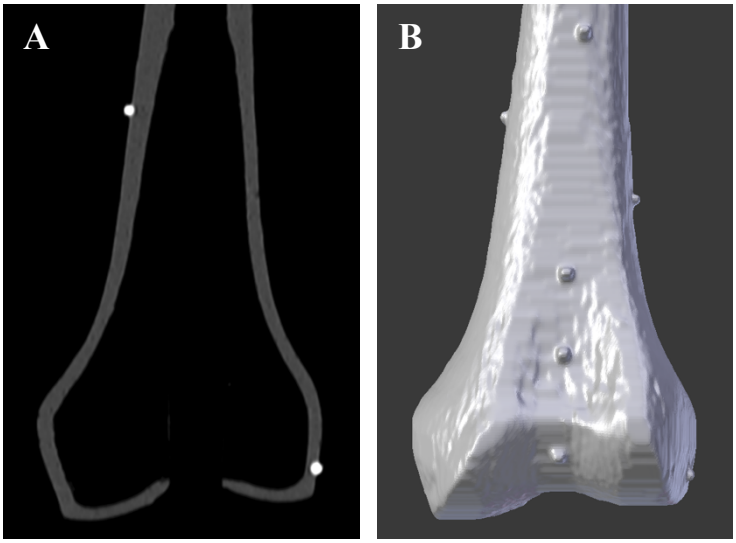

Figure 2.2. CT image of the Sawbones femur with virtual surface rendering. (A) Coronal CT image shows registration and target fiducial markers. (B) Virtual image produced via segmentation of the CT images.

Blender was utilized to perform a Boolean subtraction between a blank template and the segmented femur model, providing a matching mask at the location of interest. This mask was adjusted for thickness before being imported into a third software program, form•Z (AutoDesSys; Columbus, OH, USA), where the guide holes were created. **Figure 2.3** shows the virtual image of the point-registration guide and femur model.

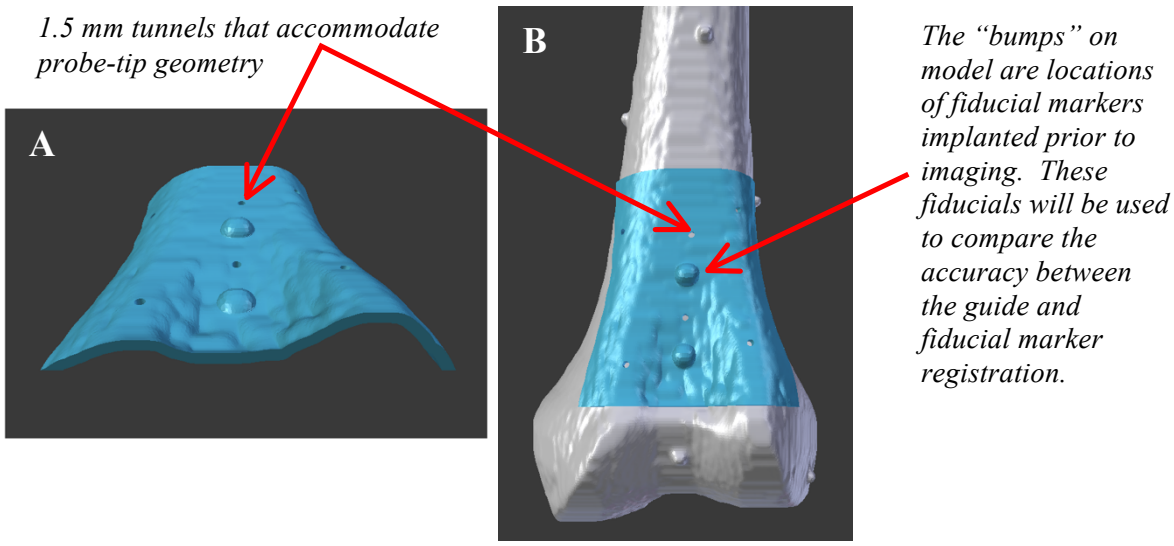

Figure 2.3. Virtual image of the patient-specific point-registration guide and femur model. (A) CAD model of a patient-specific point-registration guide that could be rapid-prototyped (3D printed) to match the anatomy of a patient's bone. (B) The surgeon would then use the tunnels to guide the navigation probe to pre-determined locations on the patient's bone during the intraoperative registration process.

The registration guide was printed by Fathom (Seattle, WA, USA) using a Stratasys (Eden Prairie, MN, USA) 3D printer and VeroClear (acrylic) plastic for $45. VeroClear plastic is meant for sterilization and thus ideal for medical applications. **Figure 2.4** shows the 3D-printed point-registration guide and Sawbones model.

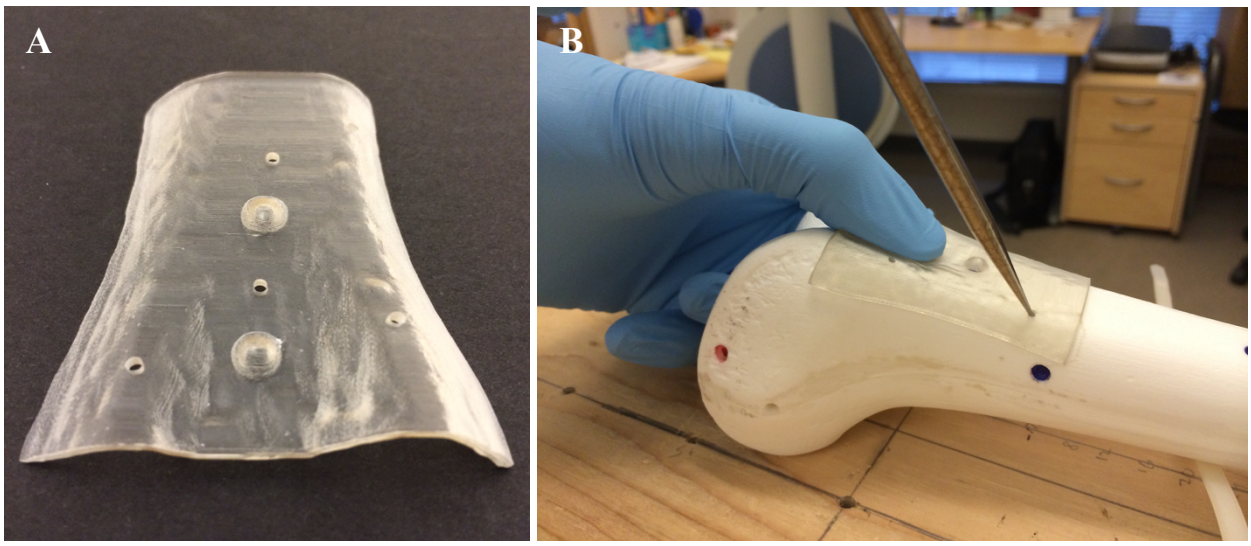

Figure 2.4. 3D-printed point-registration guide and Sawbones model. (A) A rapid-prototyped (3D printed) point-registration guide printed using the CAD model from **Figure 2.3**. (B) Point-registration guide positioned on a Sawbones model of distal femur with navigation probe tip positioned in one of the tunnels.

2.1.3 *Experimental Setup*

Image-based surgical navigation requires several steps before intraoperative registration can commence and these were simulated in the laboratory. The CT study was imported into the OrthoMap 3D Navigation Software (Stryker; Kalamazoo, MI, USA) and registration and target points marked on the virtual image (**Figure 2.5**). For fiducial registration, as well as target assessment, selections were located at the center of each of the 4 mm beads, while points chosen for anatomical landmark and 3D-printed guide registration were on the surface of the Sawbones model. As previously mentioned, anatomic landmarks included the medial and lateral epicondyles, and deepest point of the trochlear groove. The DICOM coordinates of each guide hole endpoint were retained and translated into the OrthoMap 3D coordinates for paired-point registration using the guide. Finally, the patient tracker (dynamic reference base with light-emitting diodes) was fixed to the proximal femur for Sawbones localization and tracking.

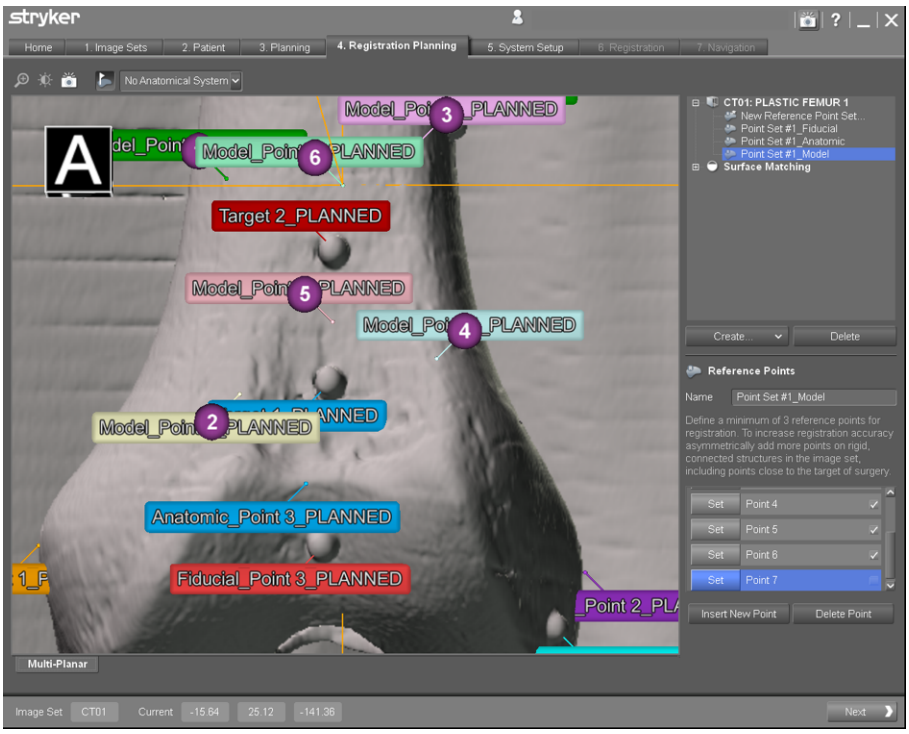

Figure 2.5. Planned registration and target points on the virtual femur model.

Points were located at the center of the 4 mm beads for fiducial localization (fiducial marker registration and target point accuracy assessment) and on the surface of the Sawbones model for selection of surface points (anatomical landmark and 3D-printed guide registration).

2.2 Inter-Observer Study: Registration and Target Accuracy

2.2.1 *Experimental Protocol*

Registration and target accuracy of the 3D-printed point-registration guide was compared with both anatomic landmark and fiducial marker registration. Paired-point registration with and without surface matching was utilized for each technique for a total of six trials. Specifically, an optically tracked pointer (utilizing light-emitting diodes) was used to perform four steps: 1) paired-point matching, 2) resampling of the three planned registration points and recording of the six target points for assessment of registration and target accuracy, 3) registration refinement using surface matching (requiring a minimum of 30 points), and 4) repetition of step 2. Paired-

point registration requires a minimum of three points and this number was selected for two reasons. First, it is difficult to identify more than three distinct anatomical landmarks in a typical distal femoral procedure and, second, it better simulates a worst-case scenario. Finally, one 4 mm diameter fiducial bead was drilled out and used as a cap for the 1.5 mm diameter Stryker pointer when the fiducial centers were the points of interest (e.g., the target points); the cap was removed for anatomic landmark and 3D-printed guide registration, as well as for surface mapping. This process was repeated by five different orthopaedic surgeons, two residents and three fellows, with varying surgical navigation experience. **Figure 2.6** shows the virtual femur with tracked pointer post-registration.

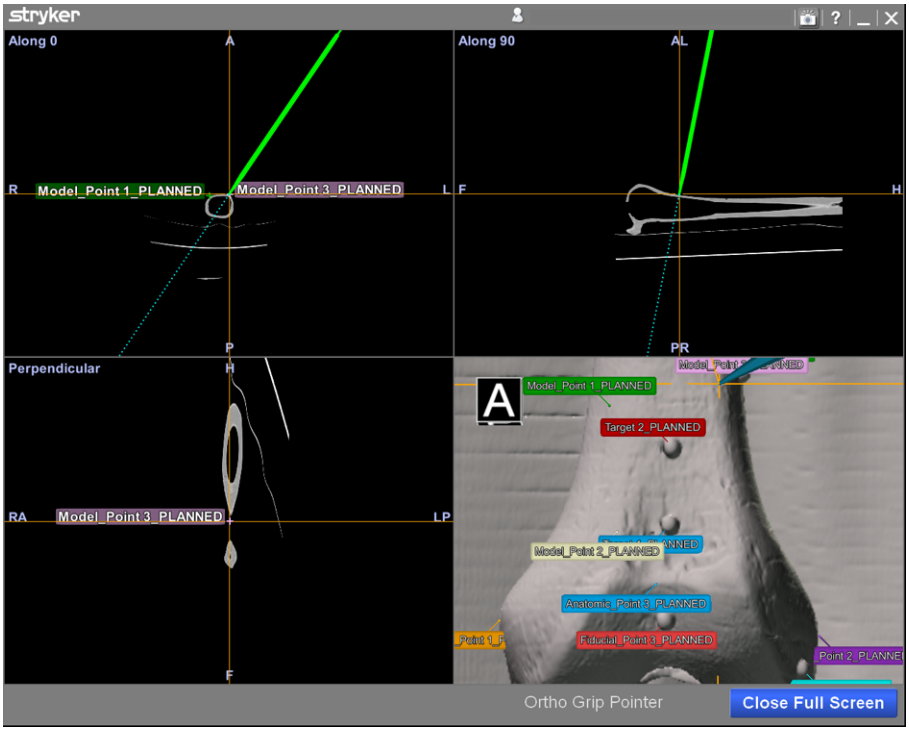

Figure 2.6. Planned registration and target points on the virtual femur model with tracked pointer post-registration.

The tracked navigation probe is pointing to one of the 3D-printed guide registration points after mapping of the physical Sawbones model with the virtual image. Registration and target points were recorded post-registration for accuracy assessments.

2.2.2 *Data and Statistics*

Registration and target accuracy were established using measurement error (ME), computed as the difference between point coordinates planned on the virtual image and those sampled post-registration. Data files were exported from the navigation system and the ME calculated using the following equation:

$$ME = \sqrt{(x_1 - x_2)^2 + (y_1 - y_2)^2 + (z_1 - z_2)^2} \quad (2.1)$$

where x_1, y_1, and z_1 are the virtually planned registration and target point coordinates, and x_2, y_2, and z_2 the corresponding post-registration coordinates.

Statistical analyses were done with the IBM Statistical Package for Social Sciences (SPSS) version 24.0. Initially, relative distributions were determined for each variable, and the data were assessed for normality and entry accuracy. Subjects with missing data were excluded from final analyses. An analysis of variance (ANOVA) and pairwise t-tests were used to assess study objectives. Comparison was made between registration techniques (i.e., anatomic landmarks, fiducial markers, and the 3D-printed guide) for both the paired-point only and paired-point with surface matching groups. Subsequent comparison was made between groups for each registration method (e.g., anatomic landmarks vs. anatomic landmarks with surface matching). Comparisons were done for both registration and target accuracy. For all analyses the alpha level was set at 0.05 with a confidence interval at the 95% level. It was hypothesized that the point-registration guide would be comparable to fiducial marker registration and both would significantly outperform anatomic landmark registration.

2.3 Intra-Observer Study: Precision

2.3.1 *Experimental Protocol*

Precision was evaluated via repeated digitization of the registration and target points (i.e., the anatomical landmarks, 3D-printed guide holes, and fiducial markers used for registration, as well as the six target points). Each point was recorded five times with both the surgical navigation and MicroScribe digitizing systems. For the Stryker Navigation System, fiducial registration without surface mapping was used to register the Sawbones prior to data collection. The femoral model was located 150 cm from the navigation system camera and all infrared markers were visible to simulate ideal working conditions. As was the case with registration and target accuracy assessment, one 4 mm diameter fiducial bead was used as a cap for both the Stryker pointer and MicroScribe tip when fiducial centers were the points of interest. All data were collected by the author (JKW).

2.3.2 *Data and Statistics*

Precision was defined as the standard deviation of the mean for 5 repeated measurements. Therefore, average 3D-coordinate locations were determined for each registration and target point cluster, followed by calculation of the mean and standard deviation of the distance to the average. Values were determined using both the Stryker Navigation System and MicroScribe. Descriptive statistics were done with SPSS version 24.0. Comparison was made between anatomic landmarks, fiducial markers, and the 3D-printed point-registration guide. It was hypothesized that repeated localization of point-registration guide points would approach the precision of fiducial marker localization, while both would outperform the precision of anatomic landmark localization.

Chapter 3. RESULTS

3.1 Inter-Observer Study: Registration Accuracy

Registration accuracy, defined as the measurement error (ME) between virtually planned registration point coordinates and those same points sampled post-registration, was calculated for each trial. The results are summarized in **Table 3.1** and **Figure 3.1**. Mean ME for paired-point registration was 2.55 ± 0.85 mm, 0.58 ± 0.24 mm, and 0.86 ± 0.38 mm when using anatomical landmarks, fiducial markers, and the 3D-printed registration guide, respectively. With surface matching, the mean errors shifted to 3.64 ± 0.64 mm, 1.08 ± 0.29 mm, and 0.99 ± 0.44 mm.

Table 3.1. Summary of anatomical landmark, fiducial, and 3D-printed guide registration accuracies.

Registration accuracy (i.e., ME between planned registration point coordinates and those sampled post-registration) was calculated for anatomical landmarks, fiducial markers, and the 3D-printed guide. Paired-point matching with and without surface mapping was utilized.

Registration Technique	Paired-point matching (mm)	Surface matching (mm)
Anatomic landmarks	2.55 ± 0.85	3.64 ± 0.64
Fiducial markers	0.58 ± 0.24	1.08 ± 0.29
3D-printed guide	0.86 ± 0.38	0.99 ± 0.44

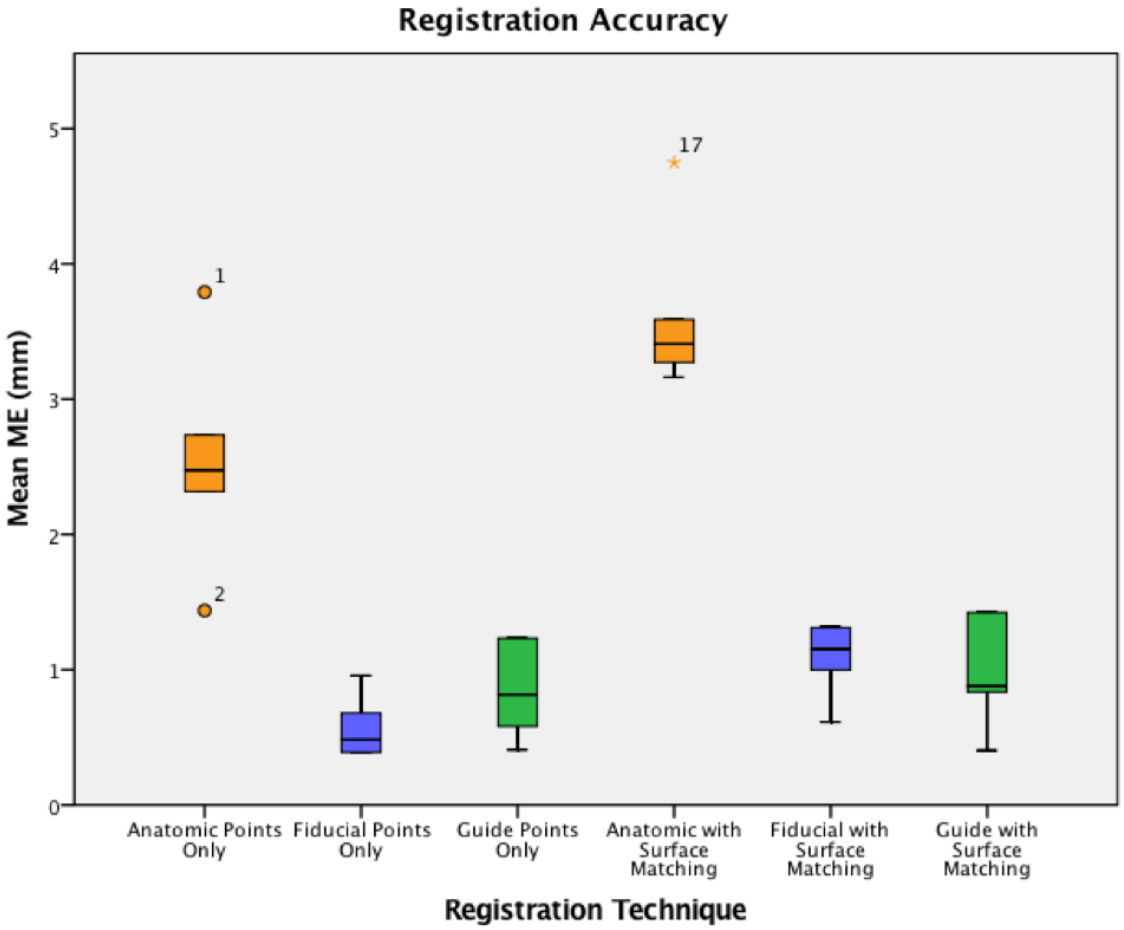

Figure 3.1. Comparison of anatomical landmark, fiducial marker, and 3D-printed guide registration accuracies.

3.1.1 *Paired-Point Matching*

One-way ANOVA for the effect of registration technique on ME was conducted for paired-point matching in the absence of surface mapping. There was significant variation in registration accuracy among the three groups ($F_{(2,12)} = 18.63$, $p < .001$), and Tukey HSD tests were utilized to assess pairwise differences. Fiducial markers significantly outperformed anatomical landmarks ($p < .001$), as did the 3D-printed guide ($p = .001$). There was no significant difference between the fiducial and guide techniques ($p = .717$). Results are shown in **Table 3.2**.

Table 3.2. Comparison of registration accuracies when using paired-point matching alone.
One-way ANOVA was used to identify a significant difference in registration accuracy among registration techniques. Tukey HSD tests were used to assess significant pairwise relationships.

Registration technique	Mean difference (mm)	*p*-value
Fiducial vs. Anatomic	-1.97	< .001
Guide vs. Anatomic	-1.70	= .001
Guide vs. Fiducial	0.28	= .717

3.1.2 *Paired-Point with Surface Matching*

A significant variation in registration accuracy remained after refinement with surface matching ($F_{(2,12)} = 49.14$, $p < .001$). Evaluation of pairwise differences showed anatomical landmarks to be significantly less accurate than both fiducial markers ($p < .001$) and the 3D-printed guide ($p < .001$). No significant difference existed between fiducial and guide registration ($p = .958$). Results are shown in **Table 3.3**.

Table 3.3. Comparison of registration accuracies when using paired-points with surface matching.
One-way ANOVA was used to identify a significant difference in registration accuracy among registration techniques. Tukey HSD tests were used to assess significant pairwise relationships.

Registration technique	Mean difference (mm)	*p*-value
Fiducial vs. Anatomic	-2.56	< .001
Guide vs. Anatomic	-2.64	< .001
Guide vs. Fiducial	-0.08	= .958

3.1.3 *Comparison of Paired-Point vs. Surface Matching*

The registration accuracies of paired-point matching and surface mapping were compared for each registration technique. A significant difference was not detected in the anatomical landmark, fiducial marker, or patient-specific guide comparisons. Results are in **Table 3.4**.

Table 3.4. Comparison of paired-point and surface matching registration accuracies within each registration technique.

Pairwise t-test comparisons were used to assess whether a significant difference was present between paired-point and surface matching registration accuracies.

Registration technique	Mean difference (mm)	$t_{(4)}$	*p*-value
Anatomic landmarks	-1.09	-1.764	.153
Fiducial markers	-0.50	-2.642	.057
3D-printed guide	-0.14	-.582	.592

3.2 Inter-Observer Study: Target Accuracy

Target accuracy was defined as the ME between virtually planned target point coordinates and those sampled post-registration. Values were calculated for each trial and the results are summarized in **Table 3.5** and **Figure 3.2**. Mean ME for paired-point registration was 5.20 ± 1.69 mm, 1.06 ± 0.26 mm, and 1.74 ± 0.66 mm when using anatomical landmarks, fiducial markers, and the 3D-printed registration guide, respectively. With surface matching, the mean target errors shifted to 1.39 ± 0.49 mm, 1.03 ± 0.42 mm, and 1.38 ± 0.60 mm.

Table 3.5. Summary of anatomical landmark, fiducial, and 3D-printed guide target accuracies.

Target accuracy (i.e., mean ME between planned target point coordinates and those sampled post-registration) was calculated for anatomical landmarks, fiducial markers, and the 3D-printed guide. Paired-point matching with and without surface mapping was utilized.

Registration Technique	Paired-point matching (mm)	Surface matching (mm)
Anatomic landmarks	5.20 ± 1.69	1.39 ± 0.49
Fiducial markers	1.06 ± 0.26	1.03 ± 0.42
3D-printed guide	1.74 ± 0.66	1.38 ± 0.60

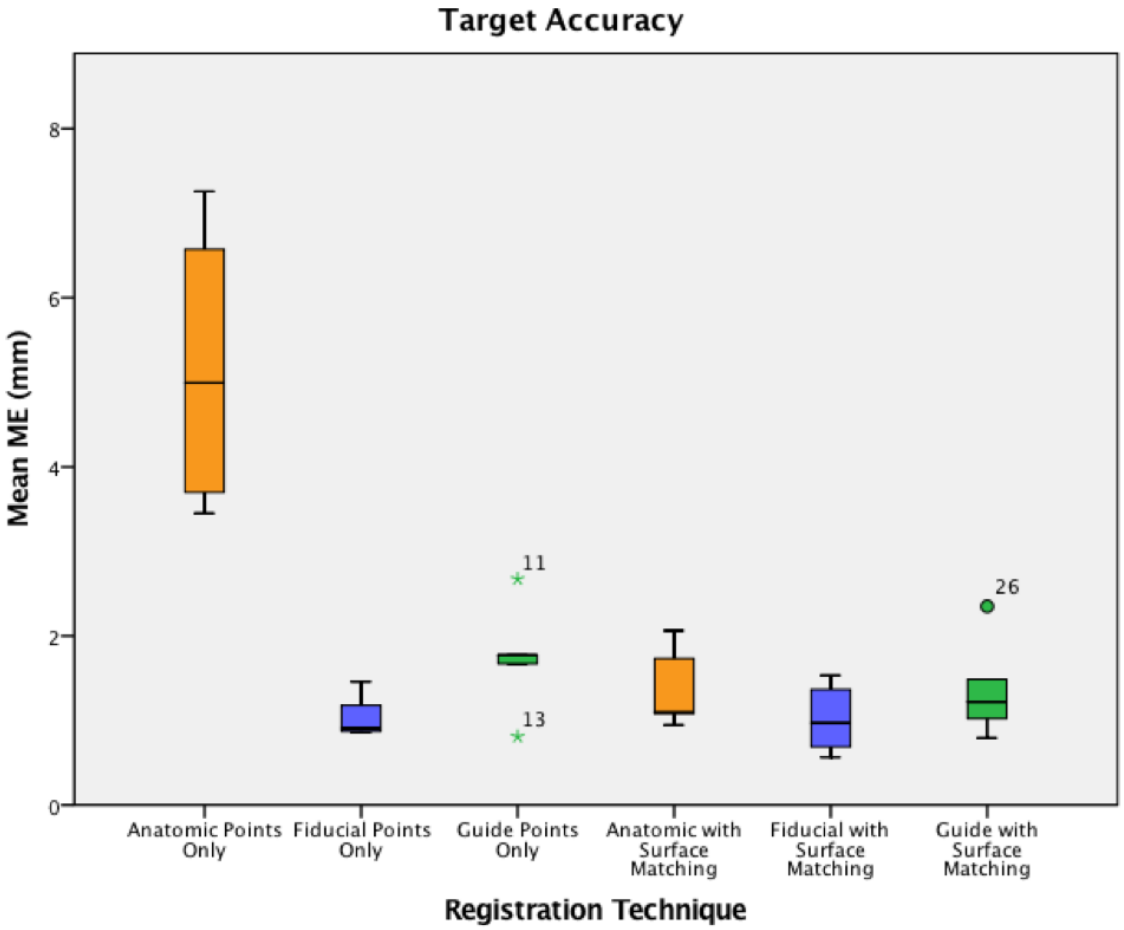

Figure 3.2. Comparison of anatomical landmark, fiducial marker, and 3D-printed guide target accuracies.

3.2.1 *Paired-Point Matching*

As with registration accuracy, paired-point matching in the absence of surface mapping resulted in a significant difference in target accuracy among the three techniques ($F_{(2,12)} = 21.89$, $p < .001$). Anatomical landmarks were significantly outperformed by both fiducial markers ($p < .001$) and the 3D-printed guide ($p = .001$). There was no significant difference between the fiducial and guide techniques ($p = .578$). Results are shown in **Table 3.6**.

Table 3.6. Comparison of target accuracies when using paired-point matching alone.
One-way ANOVA was used to identify a significant difference in registration accuracy among registration techniques. Tukey HSD tests were used to assess significant pairwise relationships.

Registration technique	Mean difference (mm)	*p*-value
Fiducial vs. Anatomic	-4.14	< .001
Guide vs. Anatomic	-3.45	= .001
Guide vs. Fiducial	0.69	= .578

3.2.2 *Paired-Point with Surface Matching*

One-way ANOVA for the effect of registration technique on ME revealed no significant difference between anatomic landmarks, fiducial markers, and the 3D-printed guide ($F_{(2,12)}$ = 0.82, p = . 466).

3.2.3 *Comparison of Paired-Point vs. Surface Matching*

Paired-point and surface matching target accuracies were compared for each registration technique. For anatomical landmarks, a significant difference was present when paired-point registration was refined with surface matching ($t_{(4)}$ = 4.622, p = .010). A significant difference in target accuracy was not found in the fiducial or guide comparisons. Results are in **Table 3.7**.

Table 3.7. Comparison of paired-point and surface matching target accuracy within each registration technique.
Pairwise t-test comparisons were used to assess whether a significant difference was present between paired-point and surface matching target accuracies.

Registration technique	Mean difference (mm)	$t_{(4)}$	*p*-value
Anatomic landmarks	3.81	4.622	.010
Fiducial markers	0.03	.180	.866
3D-printed guide	-0.14	.399	.110

3.3 Intra-Observer Study: Precision

For precision, the standard deviation of the mean for multiple (5) repeated measures was used as the primary outcome variable. Fiducial marker localization proved more precise than localization of 3D-printed guide points, while both methods outperformed anatomic landmark localization. This result was found when using both the reference measurement system (MicroScribe) and navigation system. **Table 3.8** summarizes the results for both the MicroScribe and Stryker Surgical Navigation System.

Table 3.8. Summary of anatomical landmark, fiducial, and 3D-printed guide precision. Precision (i.e., standard deviation of the repeated measures to the mean) was calculated for anatomical landmarks, fiducial markers, and 3D-printed guide points.

Method used to localize points	**Std Dev (mm)**	
	MicroScribe	**Navigation System**
Anatomic landmarks	0.3200	0.4920
Fiducial markers	0.0407	0.1635
3D-printed guide	0.1043	0.2566

Chapter 4. DISCUSSION

A patient-specific point-registration guide was developed for accurate and rapid surgical navigation registration. An anatomic Sawbones model was used to gain baseline data on the registration and target accuracies, as well as precision, of anatomical landmarks, fiducial markers, and the 3D-printed point-registration guide in an idealized model with no soft-tissue artifact. The study tested two hypotheses: 1) the point-registration guide would approach the registration and target accuracies achieved with fiducial marker registration, while both would significantly outperform anatomic landmark registration; and 2) localization of the 3D-printed guide points would be nearly as precise as fiducial marker localization, with both methods surpassing the precision of anatomic landmark localization.

4.1 Inter-Observer Study: Registration and Target Accuracy

The 3D-printed guide performed as well as fiducial marker registration in both registration and target accuracy comparisons. Refinement with surface matching did not significantly alter results for either approach. Both techniques significantly outperformed anatomical landmark registration in registration accuracy – with or without surface matching – and target accuracy for paired-point matching in the absence of surface mapping. Surface matching did, however, significantly improve the target accuracy of anatomical landmark registration. To a certain degree this result is unsurprising, as the surface point cloud is likely to overwhelm the prior paired-point registration. While this result suggests that refinement with surface mapping has the potential to equalize the various point-based registration approaches, application of this method in the operative setting can be challenging (Stoll et al., 2015). An alternative is needed and the results of this study show the patient-specific guide to be accurate in an idealized setting and worthy of further exploration.

4.2 Intra-Observer Study: Precision

As expected, localization of registration guide points proved reasonably precise in comparison to fiducial marker localization, with both methods performing better than anatomic landmark localization. Furthermore, the Stryker Navigation System performed admirably relative to the reference measurement system (MicroScribe), at least in an idealized scenario with all infrared markers visible and the femoral model placed 150 cm from the navigation system camera. Results with both the navigation system and MicroScribe demonstrate the 3D-printed guide to be sufficiently precise to warrant further evaluation.

4.3 Target Registration Error (TRE) in the Literature

Whereas registration accuracy is easier to measure and often used to estimate the effectiveness of the image-to-patient registration process, there is no statistical correlation between it and target accuracy, the commonly accepted measure of image-guided surgical accuracy (Fitzpatrick, 2010). Target accuracy is most often referred to in the surgical navigation literature as target registration error (TRE) and is utilized as a validation endpoint. The studies summarized below have similar designs to the methods outlined above in the present study. Each makes use of one or more fiducial or marker targets that are visualized on the virtual image and independent of the registration points. TRE is used as the outcome validation measure and all studies are concerned with navigation around rigid bony structures.

4.3.1 *Anatomical Landmarks, Fiducial Markers, and Surface Point Clouds*

Numerous studies encompassing neurological, oral and maxillofacial, and otolaryngology-head and neck (ENT) surgical applications have looked at TRE in the context of anatomical landmark, fiducial, and surface point cloud registration (**Table 4.1**). Generally, invasive fiducial markers

performed best. Anatomical landmarks and surface matching performed relatively well in phantom studies, but as expected, cadaver studies seemed to indicate a noticeable drop-off when soft tissue structures were present.

4.3.2 *Dental Splint Registration Devices*

Registration templates based on a modified dental splint are often used in oral and maxillofacial, and otolaryngology-head and neck (ENT), image-guided surgery. The forerunner to the patient-specific registration guide, the dental splint includes a mouthpiece, as well as fiducial screws inserted directly into the mouthpiece or an attached fiducial frame for paired-point registration. The patient is scanned with the splint in place, which is later refitted during the surgical procedure for registration and tracking. **Table 4.2** summarizes device validation in the literature.

The dental splint has generally been shown to be comparable to fiducial marker registration in TRE assessment studies. However, an important qualification exists. As noted by Eggers et al. in their examination of the device for surgery in the midface, skull base, and cranial vault, the template was effective for targets near the dental splint, but accuracy decreased significantly as the target moved away from the registration locale (Georg Eggers, Mühling, & Marmulla, 2005; Georg Eggers & Mühling, 2007). Others have found poor results outside the midface, as well as a marked decrease in performance with distance from the reference markers (Bettschart et al., 2012; Grauvogel, Soteriou, Metzger, Berlis, & Maier, 2010; Luebbers et al., 2008). While not entirely surprising, it does reiterate the importance of using registration points near the target location.

Table 4.1. TRE in the literature: anatomical landmark, fiducial marker, and surface registration techniques.

Location	Study design	Intraoperative data source	Mean TRE (mm)
Midface, skull base, and cranial vault (Ahmadian, Fathi Kazerooni, Mohagheghi, Amini Khoiy, & Sadr Hosseini, 2014)	Phantom	Invasive fiducials	0.25 – 1.15
Midface, skull base, and cranial vault (Grauvogel, Grauvogel, Arndt, Berlis, & Maier, 2012)	Phantom	Surface point cloud	1.30 – 1.46
Skull base and cranial vault (Hoffmann, Westendorff, Leitner, Bartz, & Reinert, 2005)	Phantom	Adhesive fiducials Surface point cloud	1.00 ± 0.15 2.08 ± 0.49
Mandible (Kang et al., 2013)	Phantom	Anatomical landmarks Invasive fiducials	1.0 – 3.5 0.7 – 3.3
Skull base and cranial vault (Makiese, Pillai, Salma, Sammet, & Ammirati, 2010; Salma, Makiese, Sammet, & Ammirati, 2012)	Cadaver	Adhesive fiducials Auto-registration mask Invasive fiducials	3.12 – 3.83 2.16 – 3.20 1.95 – 2.91
Temporal bone (Pillai, Sammet, & Ammirati, 2008)	Cadaver	Invasive fiducials	0.83 ± 0.11
Midface and cranial vault (Schicho et al., 2007)	Cadaver	Invasive fiducials Surface point cloud	1.4 3.0
Midface, skull base, and cranial vault (Serej, Ahmadian, Mohagheghi, & Sadrehosseini, 2015)	Phantom	Anatomical landmarks Surface point cloud #1 Surface point cloud #2	1.95 – 3.50 1.65 – 2.57 0.89 – 1.44
Midface and skull base (Sun et al., 2013)	Phantom	Anatomical landmarks	0.93 – 1.25
Skull base and cranial vault (Woerdeman, Willems, Noordmans, Tulleken, & van der Sprenkel, 2007)	Phantom	Adhesive fiducials Invasive fiducials Surface point cloud	1.37 ± 0.66 1.58 ± 0.71 1.64 ± 0.78

Table 4.2. TRE in the literature: dental splint registration devices.

Location	Study design	Intraoperative data source	Mean TRE (mm)
Mandible, midface, skull base, and cranial vault (Bettschart et al., 2012)	Phantom	Dental splint #1 Dental splint #2	2.07 ± 0.78 1.53 ± 0.55
Midface, skull base, and cranial vault (Georg Eggers et al., 2005; Georg Eggers & Mühling, 2007; Georg Eggers, Senoo, Kane, & Mühling, 2009)	Phantom	Dental splint	0.7 – 5.6
Midface, skull base, and cranial vault (Grauvogel et al., 2010)	Phantom	Dental splint Invasive fiducials Surface point cloud	0.98 ± 0.16 0.67 ± 0.11 1.3 ± 0.12
Temporal bone (Hofer et al., 2010)	Phantom	Dental splint Invasive fiducials	1.34 0.48
Temporal bone (Labadie et al., 2005)	Cadaver	Dental splint	0.73 ± 0.25
Lateral skull base (Ledderose, Hagedorn, Spiegl, Leunig, & Stelter, 2012)	Cadaver	Dental splint Invasive fiducials Surface point cloud	0.55 ± 0.28 0.33 ± 0.26 1.91 ± 0.74
Midface, skull base, and cranial vault (Luebbers et al., 2008)	Phantom	Dental splint Invasive fiducials Splint + fiducials Surface point cloud	1.1 – 2.3 0.7 – 1.1 0.6 – 1.2 1.0 – 1.2
Midface and cranial vault (Metzger, Rafii, Holhweg-Majert, Pham, & Strong, 2007; Strong, Rafii, Holhweg-Majert, Fuller, & Metzger, 2008)	Cadaver	Anatomical landmarks Dental splint Invasive fiducials Surface point cloud	1.57 – 3.17 2.93 – 4.09 1.00 – 1.34 1.81 – 2.03
Midface, skull base, and cranial vault (Venosta et al., 2014)	Phantom	Dental splint #1 Dental splint #2	1.50 – 2.86 1.76 – 2.33
Mandible and maxilla (Widmann et al., 2010)	Phantom	Dental splint #1 Dental splint #2 Invasive fiducials	0.93 ± 0.36 0.94 ± 0.40 0.94 ± 0.37
Midface, skull base, cranial vault (Zhang, Wang, Yu, Liu, & Shen, 2011; Zhang et al., 2012)	Cadaver	Dental splint Invasive fiducials	0.56 – 0.96 0.93 – 3.19

4.3.3 *Patient-Specific Registration Guides*

The patient-specific registration guide, rapid prototyped from 3D mesh information available in the preoperative imaging data, offers the potential for extension of the dental splint registration concept to locations outside the midface. Matsumoto et al. first developed the idea for use in otolaryngology-head and neck (ENT) surgery, and in a preliminary study were able to generate target accuracies similar to those found in fiducial registration (Matsumoto et al., 2009). They would later report satisfactory results using the technique for cochlear implantation (Matsumoto et al., 2012); however, surgeons found the method to be complex and time consuming, leading them to further automate the process with similar effectiveness (Oka et al., 2014; Yamashita et al., 2016). Another group developed a similar concept for total knee arthroplasty and found a maximum guide attachment error of 0.321 mm in a cow model, although they did not test the device in a clinical simulation (Jang & Lee, 2014). **Table 4.3** summarizes TRE simulation studies in the literature.

Table 4.3. TRE in the literature: the patient-specific registration guide.

Location	**Study design**	**Intraoperative data source**	**Mean TRE (mm)**
Temporal bone (Matsumoto et al., 2009)	Phantom	Adhesive fiducials	1.38 – 2.65
		Anatomical landmarks	2.18 – 6.17
		Dental splint	2.97 – 3.64
		Fiducials + landmarks	0.96 – 3.14
		Patient-specific registration guide	0.92 – 3.07
Temporal bone (Oka et al., 2014)	Phantom	Patient-specific registration guide (version 1)	1.2 ± 0.12
		Patient-specific registration guide (version 2)	0.89 – 1.04

4.3.4 *Summary*

Table 4.4 provides a summary of the mean TREs found in the aforementioned studies.

Table 4.4. Summary of the mean TREs found in the literature.

Intraoperative data source	**Mean TRE (mm)**	
	Phantom studies	**Cadaver studies**
Invasive fiducials	0.25 – 3.3	0.33 – 3.19
Adhesive fiducials	1.00 – 2.65	3.12 – 3.83
Anatomic landmarks	0.93 – 6.17	1.57 – 3.17
Surface point cloud	0.89 – 2.57	1.81 – 3.0
Auto-registration mask		2.16 – 3.20
Dental splint registration device	0.7 – 5.6	0.55 – 4.09
Patient-specific registration guide	0.89 – 3.07	

4.4 Study Limitations and Implications

While implanted fiducial markers are the gold standard for image-guided surgical registration, they either require an extra procedure or intraoperative imaging that add time, cost, and in some cases, radiation exposure to the course of care. Therefore, it is imperative to find an alternative that reduces the burden on patient, clinician, and the health care system. Paired-point matching using anatomical landmarks and surface mapping have been used as alternatives, but distinct landmarks or surfaces are needed for their effectiveness. The patient-specific point-registration guide was developed for use in applications where anatomical landmarks and surface matching are unreliable or ineffective.

The present work shows the potential of the 3D-printed point-registration guide; however, the study did have several limitations. First, while use of a Sawbones model was helpful in establishing baseline accuracy and precision, there needs to be a cadaver study to fully understand the effects of soft tissues on the various registration techniques. Also, it is difficult for a laboratory study to effectively simulate all the elements present in the OR. Anatomical

changes may occur between preoperative scan and intraoperative execution (e.g., alteration of tumor bulk and composition with subsequent displacement of anatomical landmarks), and larger managerial stressors are often present that cannot be accounted for in this type of study. Third, the patient-specific registration guide requires exposure of part of the bone during surgery. This requirement is not an issue with many sarcoma-related surgeries, where large portions of bone are often exposed prior to resection, but would not be appropriate for minimally invasive approaches, or soft tissues tumors without bony involvement. Another limitation of the study pertains to the use of CT as the image map. While many orthopaedic procedures utilize CT as the standard of care, this is not always the case with sarcoma. MRI is often the modality of choice, meaning CT is only necessary for surgical navigation. Therefore, extension of the technique to MRI-based image data would go a long way towards eliminating the need for CT-based navigation when deemed unnecessary or inappropriate. Finally, while the guide might very well lower the cost associated with image-guided surgery, surgical navigation technology is typically only available in larger medical centers and hospitals, which could ultimately limit adoption.

Despite these limitations, the study findings have significant implications for surgical navigation applications. The 3D-printed registration guide performed well in comparison to fiducial marker registration, suggesting the possibility of adequate alignment without the need of an extra scan and/or procedure. Thus, successful translation to the clinical setting will likely remove or lower appreciable time and cost constraints, as well as reduce the risk of radiation-induced conditions and surgical complications such as post-operative infection. Increased precision and accuracy will also decrease the potential for reoperation due to inadequate tumor resection margins or implant malalignment. These outcomes, combined with the easing of registration-associated barriers to surgical navigation adoption, will possibly lead to greater

confidence and acceptance of the technology. For instance, registration using anatomic landmarks typically takes 5 minutes for an orthopedic oncology procedure at SCH. The guide is expected to reduce this time to under a minute. Finally, as a technique that aids in the integration of preoperative planning with intraoperative execution and postoperative assessment, the registration guide may help further streamline the operative workflow with a reduction of OR time and associated costs. However, the extent of savings will depend on the cost attached to producing registration guides (e.g., tech time and 3D printing costs). Therefore, this benefit might be limited, at least until the technique can be scaled.

This study provided baseline accuracy and precision data on the patient-specific registration guide in an idealized Sawbones model. Furthermore, a process was developed for producing the registration guides from CT imaging. Preliminary results are encouraging and additional research and development is encouraged. Future studies should work towards transferring the technique to a more clinically relevant setting (e.g., cadaver and clinical trials), as well as further refinement of the process for producing the guides.

Chapter 5. CONCLUSIONS

Biomedical innovation is both technological advancement and development of technique. Thus, the would-be innovator must not merely create, but design with the end user or core purpose in mind. The quality of healthcare has improved dramatically over the last century, but this change has been accompanied by an exponential increase in cost. While there are myriad reasons for this development, it has become more and more obvious that the future of healthcare depends on greater integration of systems, disciplines, and technologies. Image-guided surgery is one tool that offers the potential for the removal of barriers, whether between diagnostic imaging and surgical intervention, or intraoperative documentation and postoperative disease management. It is not merely another technological tool; rather, it offers the opportunity for greater integration of a part of the healthcare ecosystem. Therefore, the patient-specific point-registration guide is not merely a new surgical navigation registration technique, it is representative of a multidisciplinary approach to design.

BIBLIOGRAPHY

Ahmadian, A., Fathi Kazerooni, A., Mohagheghi, S., Amini Khoiy, K., & Sadr Hosseini, M. (2014). A region-based anatomical landmark configuration for sinus surgery using image guided navigation system: a phantom-study. *Journal of Cranio-Maxillo-Facial Surgery: Official Publication of the European Association for Cranio-Maxillo-Facial Surgery*, *42*(6), 816–824. https://doi.org/10.1016/j.jcms.2013.11.019

Bettschart, C., Kruse, A., Matthews, F., Zemann, W., Obwegeser, J. A., Grätz, K. W., & Lübbers, H.-T. (2012). Point-to-point registration with mandibulo-maxillary splint in open and closed jaw position. Evaluation of registration accuracy for computer-aided surgery of the mandible. *Journal of Cranio-Maxillo-Facial Surgery: Official Publication of the European Association for Cranio-Maxillo-Facial Surgery*, *40*(7), 592–598. https://doi.org/10.1016/j.jcms.2011.10.016

Burrows, E. H. (1986). *Pioneers and early years: a history of British radiology*. St Anne, Alderney, Channel Islands: Colophon.

Ching, R. P., White, J. K., & Conrad, E. U. (2016, April 14). Patient-specific guides to improve point registration accuracy in surgical navigation. Retrieved from http://www.google.com/patents/US20160100773

Cleary, K., & Peters, T. M. (2010). Image-guided interventions: technology review and clinical applications. *Annual Review of Biomedical Engineering*, *12*, 119–142. https://doi.org/10.1146/annurev-bioeng-070909-105249

Eggers, G., & Mühling, J. (2007). Template-based registration for image-guided skull base surgery. *Otolaryngology--Head and Neck Surgery: Official Journal of American*

Academy of Otolaryngology-Head and Neck Surgery, *136*(6), 907–913. https://doi.org/10.1016/j.otohns.2006.12.021

Eggers, G., Mühling, J., & Marmulla, R. (2005). Template-based registration for image-guided maxillofacial surgery. *Journal of Oral and Maxillofacial Surgery: Official Journal of the American Association of Oral and Maxillofacial Surgeons*, *63*(9), 1330–1336. https://doi.org/10.1016/j.joms.2005.05.312

Eggers, G., Mühling, J., & Marmulla, R. (2006). Image-to-patient registration techniques in head surgery. *International Journal of Oral and Maxillofacial Surgery*, *35*(12), 1081–1095. https://doi.org/10.1016/j.ijom.2006.09.015

Eggers, G., Senoo, H., Kane, G., & Mühling, J. (2009). The accuracy of image guided surgery based on cone beam computer tomography image data. *Oral Surgery, Oral Medicine, Oral Pathology, Oral Radiology, and Endodontics*, *107*(3), e41-48. https://doi.org/10.1016/j.tripleo.2008.10.022

Fitzpatrick, J. M. (2010). The role of registration in accurate surgical guidance. *Proceedings of the Institution of Mechanical Engineers. Part H, Journal of Engineering in Medicine*, *224*(5), 607–622.

Friets, E. M., Strohbehn, J. W., Hatch, J. F., & Roberts, D. W. (1989). A frameless stereotaxic operating microscope for neurosurgery. *IEEE Transactions on Biomedical Engineering*, *36*(6), 608–617. https://doi.org/10.1109/10.29455

Galloway, R. L. (2001). The process and development of image-guided procedures. *Annual Review of Biomedical Engineering*, *3*, 83–108. https://doi.org/10.1146/annurev.bioeng.3.1.83

Galloway, R. L., Edwards, C. A., Lewis, J. T., & Maciunas, R. J. (1993). Image display and surgical visualization in interactive image-guided neurosurgery. *Optical Engineering*, *32*(8), 1955–1962. https://doi.org/10.1117/12.143712

Grauvogel, T. D., Grauvogel, J., Arndt, S., Berlis, A., & Maier, W. (2012). Is there an equivalence of non-invasive to invasive referenciation in computer-aided surgery? *European Archives of Oto-Rhino-Laryngology: Official Journal of the European Federation of Oto-Rhino-Laryngological Societies (EUFOS): Affiliated with the German Society for Oto-Rhino-Laryngology - Head and Neck Surgery*, *269*(10), 2285–2290. https://doi.org/10.1007/s00405-012-2023-6

Grauvogel, T. D., Soteriou, E., Metzger, M. C., Berlis, A., & Maier, W. (2010). Influence of different registration modalities on navigation accuracy in ear, nose, and throat surgery depending on the surgical field. *The Laryngoscope*, *120*(5), 881–888. https://doi.org/10.1002/lary.20867

Gundle, K. R., White, J. K., Conrad, E. U., 3rd, & Ching, R. P. (2017). Accuracy and precision of a surgical navigation system: effect of camera and patient tracker position and number of active markers. *The Open Orthopaedics Journal*, *11*(1).

Hajnal, J. V., Hawkes, D. J., & Hill, D. L. G. (2001). *Medical image registration*. Boca Raton: CRC Press.

Hofer, M., Dittrich, E., Baumberger, C., Strauss, M., Dietz, A., Lüth, T., & Strauss, G. (2010). The influence of various registration procedures upon surgical accuracy during navigated controlled petrous bone surgery. *Otolaryngology--Head and Neck Surgery: Official Journal of American Academy of Otolaryngology-Head and Neck Surgery*, *143*(2), 258–262. https://doi.org/10.1016/j.otohns.2010.04.021

Hoffmann, J., Westendorff, C., Leitner, C., Bartz, D., & Reinert, S. (2005). Validation of 3D-laser surface registration for image-guided cranio-maxillofacial surgery. *Journal of Cranio-Maxillo-Facial Surgery: Official Publication of the European Association for Cranio-Maxillo-Facial Surgery*, *33*(1), 13–18. https://doi.org/10.1016/j.jcms.2004.10.001

Horsley, V., & Clarke, R. H. (1908). The structure and functions of the cerebellum examined by a new method. *Brain*, *31*(1), 45–124. https://doi.org/10.1093/brain/31.1.45

Jang, T., & Lee, K. (2014). A novel registration method for computer-assisted total knee arthroplasty using a patient-specific registration guide. *Surgical Innovation*, *21*(1), 80–89. https://doi.org/10.1177/1553350613505917

Kang, S.-H., Kim, M.-K., Kim, J.-H., Park, H.-K., Lee, S.-H., & Park, W. (2013). The validity of marker registration for an optimal integration method in mandibular navigation surgery. *Journal of Oral and Maxillofacial Surgery: Official Journal of the American Association of Oral and Maxillofacial Surgeons*, *71*(2), 366–375. https://doi.org/10.1016/j.joms.2012.03.037

Kosugi, Y., Watanabe, E., Goto, J., Watanabe, T., Yoshimoto, S., Takakura, K., & Ikebe, J. (1988). An articulated neurosurgical navigation system using MRI and CT images. *IEEE Transactions on Biomedical Engineering*, *35*(2), 147–152. https://doi.org/10.1109/10.1353

Labadie, R. F., Shah, R. J., Harris, S. S., Cetinkaya, E., Haynes, D. S., Fenlon, M. R., … Fitzpatrick, J. M. (2005). In vitro assessment of image-guided otologic surgery: submillimeter accuracy within the region of the temporal bone. *Otolaryngology--Head and Neck Surgery: Official Journal of American Academy of Otolaryngology-Head and Neck Surgery*, *132*(3), 435–442. https://doi.org/10.1016/j.otohns.2004.09.141

Ledderose, G. J., Hagedorn, H., Spiegl, K., Leunig, A., & Stelter, K. (2012). Image guided surgery of the lateral skull base: testing a new dental splint registration device. *Computer Aided Surgery: Official Journal of the International Society for Computer Aided Surgery*, *17*(1), 13–20. https://doi.org/10.3109/10929088.2011.632783

Liao, R., Zhang, L., Sun, Y., Miao, S., & Chefd'hotel, C. (2013). A review of recent advances in registration techniques applied to minimally invasive therapy. *IEEE Transactions on Multimedia*, *15*(5), 983–1000. https://doi.org/10.1109/TMM.2013.2244869

Luebbers, H.-T., Messmer, P., Obwegeser, J. A., Zwahlen, R. A., Kikinis, R., Graetz, K. W., & Matthews, F. (2008). Comparison of different registration methods for surgical navigation in cranio-maxillofacial surgery. *Journal of Cranio-Maxillo-Facial Surgery: Official Publication of the European Association for Cranio-Maxillo-Facial Surgery*, *36*(2), 109–116. https://doi.org/10.1016/j.jcms.2007.09.002

Maciunas, R. J., Galloway, R. L., Fitzpatrick, J. M., Mandava, V. R., Edwards, C. A., & Allen, G. S. (1992). A universal system for interactive image-directed neurosurgery. *Stereotactic and Functional Neurosurgery*, *58*(1–4), 108–113.

Makiese, O., Pillai, P., Salma, A., Sammet, S., & Ammirati, M. (2010). Accuracy validation in a cadaver model of cranial neuronavigation using a surface autoregistration mask. *Neurosurgery*, *67*(3 Suppl Operative), ons85-90; discussion ons90. https://doi.org/10.1227/01.NEU.0000383751.63835.2F

Markelj, P., Tomaževič, D., Likar, B., & Pernuš, F. (2012). A review of 3D/2D registration methods for image-guided interventions. *Medical Image Analysis*, *16*(3), 642–661. https://doi.org/10.1016/j.media.2010.03.005

Matsumoto, N., Hong, J., Hashizume, M., & Komune, S. (2009). A minimally invasive registration method using surface template-assisted marker positioning (STAMP) for image-guided otologic surgery. *Otolaryngology--Head and Neck Surgery: Official Journal of American Academy of Otolaryngology-Head and Neck Surgery*, *140*(1), 96–102. https://doi.org/10.1016/j.otohns.2008.10.005

Matsumoto, N., Oka, M., Cho, B., Hong, J., Jinnouchi, M., Ouchida, R., … Komune, S. (2012). Cochlear implantation assisted by noninvasive image guidance. *Otology & Neurotology: Official Publication of the American Otological Society, American Neurotology Society [and] European Academy of Otology and Neurotology*, *33*(8), 1333–1338. https://doi.org/10.1097/MAO.0b013e318268d1e9

Metzger, M. C., Rafii, A., Holhweg-Majert, B., Pham, A. M., & Strong, B. (2007). Comparison of 4 registration strategies for computer-aided maxillofacial surgery. *Otolaryngology--Head and Neck Surgery: Official Journal of American Academy of Otolaryngology-Head and Neck Surgery*, *137*(1), 93–99. https://doi.org/10.1016/j.otohns.2007.02.015

Oka, M., Cho, B., Matsumoto, N., Hong, J., Jinnouchi, M., Ouchida, R., … Hashizume, M. (2014). A preregistered STAMP method for image-guided temporal bone surgery. *International Journal of Computer Assisted Radiology and Surgery*, *9*(1), 119–126. https://doi.org/10.1007/s11548-013-0916-5

Pillai, P., Sammet, S., & Ammirati, M. (2008). Application accuracy of computed tomography-based, image-guided navigation of temporal bone. *Neurosurgery*, *63*(4 Suppl 2), 326-332-333. https://doi.org/10.1227/01.NEU.0000316429.19314.67

Roberts, D. W., Strohbehn, J. W., Hatch, J. F., Murray, W., & Kettenberger, H. (1986). A frameless stereotaxic integration of computerized tomographic imaging and the operating

microscope. *Journal of Neurosurgery*, *65*(4), 545–549. https://doi.org/10.3171/jns.1986.65.4.0545

Rowland, S. (1896). Report on the application of the new photography to medicine and surgery. *British Medical Journal*, *1*(1838), 748–750.

Salma, A., Makiese, O., Sammet, S., & Ammirati, M. (2012). Effect of registration mode on neuronavigation precision: an exploration of the role of random error. *Computer Aided Surgery: Official Journal of the International Society for Computer Aided Surgery*, *17*(4), 172–178. https://doi.org/10.3109/10929088.2012.691992

Schicho, K., Figl, M., Seemann, R., Donat, M., Pretterklieber, M. L., Birkfellner, W., … Ewers, R. (2007). Comparison of laser surface scanning and fiducial marker-based registration in frameless stereotaxy. Technical note. *Journal of Neurosurgery*, *106*(4), 704–709. https://doi.org/10.3171/jns.2007.106.4.704

Serej, N. D., Ahmadian, A., Mohagheghi, S., & Sadrehosseini, S. M. (2015). A projected landmark method for reduction of registration error in image-guided surgery systems. *International Journal of Computer Assisted Radiology and Surgery*, *10*(5), 541–554. https://doi.org/10.1007/s11548-014-1075-z

Spiegel, E. A., Wycis, H. T., Marks, M., & Lee, A. J. (1947). Stereotaxic apparatus for operations on the human brain. *Science (New York, N.Y.)*, *106*(2754), 349–350. https://doi.org/10.1126/science.106.2754.349

Stoll, K. E., Miles, J. D., White, J. K., Punt, S. E. W., Conrad, E. U., 3rd, & Ching, R. P. (2015). Assessment of registration accuracy during computer-aided oncologic limb-salvage surgery. *International Journal of Computer Assisted Radiology and Surgery*, *10*(9), 1469–1475. https://doi.org/10.1007/s11548-014-1146-1

Strong, E. B., Rafii, A., Holhweg-Majert, B., Fuller, S. C., & Metzger, M. C. (2008). Comparison of 3 optical navigation systems for computer-aided maxillofacial surgery. *Archives of Otolaryngology--Head & Neck Surgery*, *134*(10), 1080–1084. https://doi.org/10.1001/archotol.134.10.1080

Sun, Y., Luebbers, H.-T., Agbaje, J. O., Schepers, S., Vrielinck, L., Lambrichts, I., & Politis, C. (2013). Validation of anatomical landmarks-based registration for image-guided surgery: an in-vitro study. *Journal of Cranio-Maxillo-Facial Surgery: Official Publication of the European Association for Cranio-Maxillo-Facial Surgery*, *41*(6), 522–526. https://doi.org/10.1016/j.jcms.2012.11.017

Venosta, D., Sun, Y., Matthews, F., Kruse, A. L., Lanzer, M., Gander, T., … Lübbers, H.-T. (2014). Evaluation of two dental registration-splint techniques for surgical navigation in cranio-maxillofacial surgery. *Journal of Cranio-Maxillo-Facial Surgery: Official Publication of the European Association for Cranio-Maxillo-Facial Surgery*, *42*(5), 448–453. https://doi.org/10.1016/j.jcms.2013.05.040

Watanabe, E., Watanabe, T., Manaka, S., Mayanagi, Y., & Takakura, K. (1987). Three-dimensional digitizer (neuronavigator): new equipment for computed tomography-guided stereotaxic surgery. *Surgical Neurology*, *27*(6), 543–547.

Widmann, G., Stoffner, R., Schullian, P., Widmann, R., Keiler, M., Zangerl, A., … Bale, R. J. (2010). Comparison of the accuracy of invasive and noninvasive registration methods for image-guided oral implant surgery. *The International Journal of Oral & Maxillofacial Implants*, *25*(3), 491–498.

Woerdeman, P. A., Willems, P. W. A., Noordmans, H. J., Tulleken, C. A. F., & van der Sprenkel, J. W. B. (2007). Application accuracy in frameless image-guided neurosurgery:

a comparison study of three patient-to-image registration methods. *Journal of Neurosurgery*, *106*(6), 1012–1016. https://doi.org/10.3171/jns.2007.106.6.1012

Yamashita, M., Matsumoto, N., Cho, B., Komune, N., Onogi, S., Lee, J., … Hashizume, M. (2016). Registration using 3D-printed rigid templates outperforms manually scanned surface matching in image-guided temporal bone surgery. *International Journal of Computer Assisted Radiology and Surgery*, *11*(11), 2119–2127. https://doi.org/10.1007/s11548-016-1441-0

Yau, W. P., Leung, A., Liu, K. G., Yan, C. H., Wong, L. L. S., & Chiu, K. Y. (2007). Interobserver and intra-observer errors in obtaining visually selected anatomical landmarks during registration process in non-image-based navigation-assisted total knee arthroplasty. *The Journal of Arthroplasty*, *22*(8), 1150–1161. https://doi.org/10.1016/j.arth.2006.10.010

Zhang, W., Wang, C., Shen, G., Wang, X., Cai, M., Gui, H., … Yang, D. (2012). A novel device for preoperative registration and automatic tracking in cranio-maxillofacial image guided surgery. *Computer Aided Surgery: Official Journal of the International Society for Computer Aided Surgery*, *17*(5), 259–267. https://doi.org/10.3109/10929088.2012.710251

Zhang, W., Wang, C., Yu, H., Liu, Y., & Shen, G. (2011). Effect of fiducial configuration on target registration error in image-guided cranio-maxillofacial surgery. *Journal of Cranio-Maxillo-Facial Surgery: Official Publication of the European Association for Cranio-Maxillo-Facial Surgery*, *39*(6), 407–411. https://doi.org/10.1016/j.jcms.2010.10.008